JCTC Journal of Chemical Theory and Computation

Article

pubs.acs.org/JCTC

Validation of the Direct-COSMO-RS Solvent Model for Diels–Alder Reactions in Aqueous Solution

Kolja Theilacker, David Buhrke, and Martin Kaupp*

Technische Universität Berlin, Institut für Chemie, Theoretische Chemie/Quantenchemie, Sekr. C7, Strasse des 17. Juni 135, 10623 Berlin, Germany

Supporting Information

ABSTRACT: The modeling of chemical reactions in protic solvents tends to be far more computationally demanding than in most aprotic solvents, where bulk solvent effects are well described by dielectric continuum solvent models. In the presence of hydrogen bonds from a protic solvent to reactants, transition states or intermediates, a faithful modeling of the solvent effects usually requires some kind of molecular dynamics treatment. In contrast, the COSMO-RS (conductor-like screening model for real solvents) approach has been known for about a decade to describe protic solvent effects much better than continuum solvents, in spite of being an implicit solvent model without explicit molecular dynamics. More recently, the self-consistent use of its potential in electronic-structure methods has led to the Direct-COSMO-RS approach. It allows, for example, structure optimization in the presence of a protic solvent, of solvent mixtures, as well as self-consistent property calculations. In view of recent successful tests for electron transfer in organic mixed-valence systems, in this work the wider applicability of D-COSMO-RS for organic reactivity is evaluated by computation of activation and reaction free energies, as well as transition-state structures of two prototypical Diels–Alder reactions, with an emphasis on aqueous solution. D-COSMO-RS indeed provides substantial improvements over the COSMO continuum model and in judicious testing compares well with embedded supermolecular model cluster treatments, without prior knowledge about the average numbers of hydrogen-bonding interactions present.

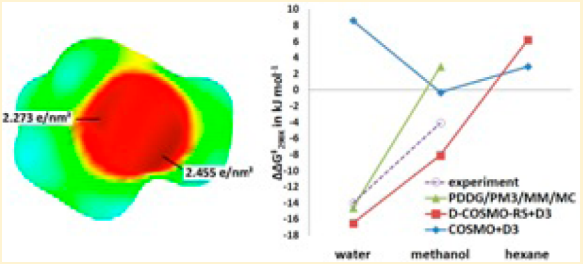

1. INTRODUCTION

As most of the technically important chemical reactions are carried out in some kind of solution environment, the quantum-chemical modeling of reactions in solution is of utmost importance in many fields. The bulk solvent effects of aprotic solvents are often most conveniently included into quantum-chemical studies by polarizable dielectric continuum models. In the absence of more specific solute–solvent interactions, these models frequently provide a reasonable description, and they have thus become the workhorse solvent models for routine applications.[1] Successful examples are the family of PCM[2,3] models or COSMO[4] (conductor-like-screening model), available in the TURBOMOLE package used in the present work.

When specific solvation effects are important, the description becomes more difficult. This holds in particular for hydrogen bonding in protic solvents like alcohols or water, which are of appreciable practical importance. Then the most accurate description is typically obtained from an explicit modeling of the solvent molecules, either in cluster models or using periodic boundary conditions. The solvent molecules may be included either quantum-chemically, which is the most accurate but also computationally most demanding approach, or by using some type of classical force field, in a QM/MM treatment. While static cluster models may to some extent capture the strongest strong solute–solvent interactions, in the majority of cases, a realistic description of the dynamical nature of the interactions requires molecular-dynamics or Monte Carlo-type simulations. While these are well-known to provide very powerful tools, it is clear that their application to chemical problems is computationally much more demanding than that of the continuum models described above.

For routine, cost-efficient applications it is thus desirable to realistically include hydrogen-bonding interactions into solvent models at essentially the cost of a continuum solvent model, that is, without the computational effort of an explicit molecular-dynamics treatment. An interesting implicit solvent model that goes beyond a polarizable continuum description with almost no extra cost is Klamt's COSMO-RS approach[3,5] (COSMO for real solvents). COSMO-RS has now been used successfully for almost two decades in an a posteriori mode, where a quantum-chemical calculation with COSMO provides the required surface charge-density distributions (σ-profiles) from which the statistical-thermodynamics ansatz of COSMO-RS constructs effective solvent chemical potentials (σ-potentials) that provide important insight into fluid-phase thermodynamics, but also into solvation free energies. Most importantly, COSMO-RS includes hydrogen-bonding terms parametrized into the σ-potential. More recently, the Direct-

Received: October 3, 2014

   dx.doi.org/10.1021/ct5008857 | J. Chem. Theory Comput. XXXX, XXX, XXX–XXX

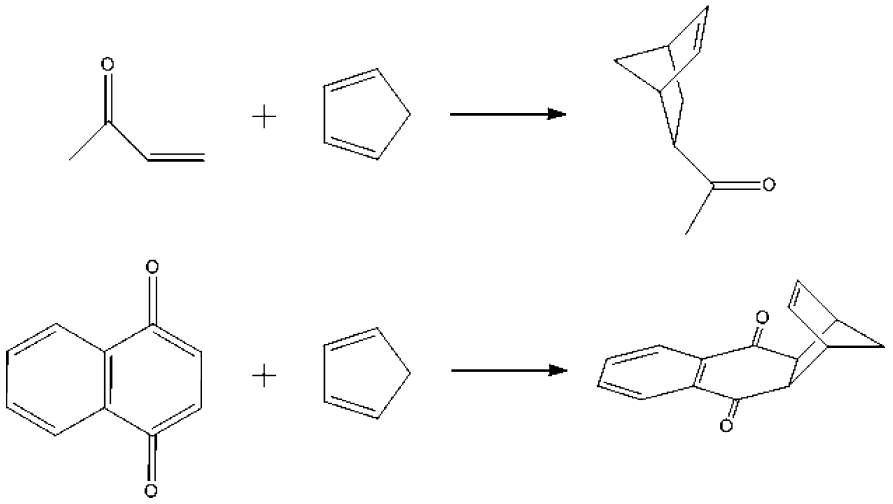

Figure 1. Two Diels–Alder reactions discussed in this work. Top MVK + CP reaction and bottom NQ + CP reaction.

COSMO-RS approach (in the following D-COSMO-RS) has been implemented, where the σ-potentials are inserted self-consistently into quantum-chemical calculations, providing for the first time a refined implicit environment of COSMO-RS quality to wave function or density-matrix optimization. Importantly, this includes molecular gradients and properties, thus allowing the influence of protic solvents on structures, energetics, and properties to be probed self-consistently. The first example of such D-COSMO-RS calculations were computations of electronic g-tensors by Klamt, Neese, and co-workers[6] using the implementation in the ORCA program package. More recently, we have used the TURBOMOLE implementation of D-COSMO-RS to demonstrate how internal electron-transfer reactions of organic mixed-valence systems may be treated.[7] Importantly, D-COSMO-RS was able to faithfully describe the differences between aprotic and protic (alcohol) solvents for the localized/delocalized nature and electron-transfer barriers of mixed-valent radical anions, including the first treatment of solvent mixtures. To establish D-COSMO-RS as a general tool for studies in protic solvents, it is important to establish that the good performance of D-COSMO-RS persists also in other fields of application. Here we extend the validation to a very different class of organic chemical reactions, namely Diels–Alder reactions in aqueous solution. We compare D-COSMO-RS results to gas-phase and COSMO data, as well as to an explicit inclusion of solvent molecules in cluster models (in part embedded in an implicit solvent). These comparisons are made to a large extent at the DFT level, using the PBE0 functional[8−12] and Grimme's D3 dispersion corrections.[13] This level is found to reproduce post-Hartree–Fock energetics in the gas phase much more faithfully than other functionals tested. The paper setup is thus as follows: after the Computational Details section, we first describe the comparison of various computational levels and basis sets for two prototypical Diels–Alder gas-phase reactions, namely those of methyl-vinyl-ketone (MVK) and 1,4-naphthoquinone (NQ), respectively, with cyclopentadiene (CP), compare Figure 1. On the basis of the outcome of the gas-phase evaluations, we subsequently use the PBE0 and PBE0-D3 levels to evaluate various approaches to include solvent effects for the same two reactions.

2. COMPUTATIONAL DETAILS

All calculations have been performed with the TURBOMOLE6.3 package,[14−16] using def2-TZVP basis sets[17] in the DFT calculations and Dunning correlation-consistent aug-cc-pVXZ-type (X = D, T, Q, 5) basis sets[18,19] for the ab initio single-point calculations. The density functionals B3LYP,[8,9,20−23] PBE0,[8−12] and BP86[8,9,20,21,24] were considered, using the resolution-of-the-identity approximation for the latter (RI-BP86). Dispersion contributions for the DFT calculations were evaluated using Grimme's DFT-D3 atom-pairwise dispersion corrections for these three functionals.[13]

Validation of the DFT functionals in the gas phase was done against single-point ab initio wave function calculations at the PBE0-D3 gas-phase structures (use of structures optimized at other levels led to only minor changes, see below). For HF, MP2, and spin-component-scaled (SCS) MP2 calculations,[25] complete-basis-set extrapolations (CBS)[26] were done with a two-point extrapolation from aug-cc-pVXZ (X = Q, 5) results. CCSD and CCSD(T) calculations were possible only up to the aug-cc-pVTZ basis-set level.

Solvent effects were taken into account in the DFT calculations at different levels: the COSMO (conductor-like-screening-model[3]) approach represents a polarizable continuum model. The following solvents have been used, with their respective dielectric constants ε: water (ε = 78.3553), hexane (ε = 1.8819), acetonitrile (ε = 35.688), and methanol (ε = 32.613). The main attention pertains to the self-consistent D-COSMO-RS ansatz. The required σ-potentials have been created with the COSMOtherm program[27] at BP86/TZVP level for 298 K. For comparison, we have also included explicit water molecules, either in gas-phase cluster models or embedded in the COSMO or D-COSMO-RS solvent environments.

All fully optimized minima and transition states have been verified by harmonic vibrational frequency analyses. It was verified that the imaginary frequency of a given transition state pertains to the reaction at hand. In the COSMO and D-COSMO-RS solvent environments, the frequency calculations had to be done by numerical differentiation of analytical gradients (using the numforce module of TURBOMOLE6.3, while aoforce was employed in the gas-phase calculations). Numerical problems of the solvent cavity models occasionally produced small extra imaginary frequencies in the frequency

dx.doi.org/10.1021/ct5008857 | J. Chem. Theory Comput. XXXX, XXX, XXX–XXX

analyses for some calculations where explicit H_2O solvent molecules were embedded in COSMO or D-COSMO-RS for the NQ+CP system (the spurious imaginary frequencies pertained to soft H_2O solvent modes). This gave rise to inaccuracies in the computed entropic contributions (see below).

While the comparison of gas-phase barriers and thermochemistry will focus on the pure electronic contributions to validate the electronic-structure methods, mainly the Gibbs free energies will be compared in solvent environments. This is preferable because (a) the separation into enthalpic and entropic contributions of the solvent contributions is not very well-defined (separate contributions provided pertain essentially to internal degrees of freedom), (b) mostly free energies are available from experiment, and (c) we may better compare our results to those of previous molecular dynamics studies. The entropies and enthalpies at 298 K were evaluated based on the output of harmonic vibrational frequency analyses at the indicated levels. In those few cases, where spurious imaginary frequencies in the vibrational calculations made the entropies unreliable for the NQ + CP reaction (see above), these were estimated from results for more successful, closely similar calculations.

We note finally, that for both reactions we concentrate exclusively on the endo addition mode that has previously been identified as the lowest-energy pathway, and on the s-cis conformation of MVK. Self-consistent COSMO and D-COSMO-RS surface charge densities have been plotted using the COSMOTherm software.[27]

3. RESULTS AND DISCUSSION

A. Validation of Density Functionals against Wave Function Methods in the Gas Phase. As preliminary calculations revealed a very large sensitivity of activation barriers and reaction energies of the two title reactions to the density functional used, we first selected the preferred DFT approach by benchmarking against gas-phase energies obtained using various post-Hartree−Fock approaches. Table 1 shows, first of all, an extremely large influence of electron correlation on both activation barriers and reaction energies, as exemplified by the differences between the post-HF and HF results. While the computational effort of coupled-cluster calculations prevented CC calculations for the NQ + CP reaction, as well as reliable extrapolation to the complete basis-set limit at the CC level for the MVK + CP reaction, MP2, and SCS-MP2 allowed us to obtain energies up to aug-cc-pV5Z basis sets for both reactions, providing an accurate CBS extrapolation (results for further individual basis-set levels are given in Table S1 in Supporting Information). We may thus estimate the CBS-limit coupled-cluster energies for the MVK reaction by assuming that the basis-set corrections from the MP2 or SCS-MP2 calculations carry over to the CC levels. Most notably, however, the SCS-MP2 and CCSD(T) energies with the aug-cc-pVTZ basis set are rather close to each other (even closer for the reaction energy than for the barrier). This suggests the direct use of the SCS-MP2/CBS data as a good estimate also for the so far unavailable CCSD(T)/CBS data. This confirms earlier validation work on SCS-MP2 for a number of related pericyclic reactions, where SCS-MP2 with extended basis sets agreed excellently with G3 or CBS-QB3 levels of theory.[28]

Increasing the basis set beyond the aug-cc-pVTZ level renders both the activation barriers and the reaction energies higher by about 15−20 kJ mol^{-1}. This suggests that the aug-cc-pVTZ basis does still cause notable basis-set superposition errors (BSSE) for the transition states and products of the two title reactions. It appears that BSSE is already small at the aug-cc-pVQZ basis level. Basis-set effects and differences between various computational levels for the NQ + CP reaction are roughly comparable to the results for the MVK + CP reaction, albeit the differences between aug-cc-pVTZ and CBS values are somewhat larger, closer to about 25 kJ mol^{-1}. We will assume in the following that the SCS-MP2/CBS data provide a good estimate of CCSD(T)/CBS quality energetics also for the NQ + CP reaction. As found earlier,[28] the SCS-MP2/CBS energies are a significant improvement over standard MP2 results, in particular for the activation barriers, where MP2 provides even negative values. The effects of triple excitations in the coupled-cluster data for the MVK + CP reaction are small (ca. −3 kJ mol^{-1}) for the reaction energy but notable (ca. −27 kJ mol^{-1}) for the barrier, consistent with a significant importance of nondynamical correlation effects at the transition state (these are also apparent from the poor performance of MP2 for the barriers).

Having thus obtained reasonable benchmark energies for the two title gas-phase reactions, we turn now to an evaluation of DFT results. The dependence on the functional, as well as on the D3 dispersion corrections, is striking for both the activation barriers and the reaction energies. While this may seem unusual given the, at first sight, simple symmetry-allowed DA-reactions chosen for the present study, the observation is well in line with previous findings. This holds in particular for the extremely poor performance of the B3LYP functional, which has been noted also for related pericyclic reactions, including DA reactions.[25,28] For example, the DARC subset[29,30] of Grimme's large GMTKN30 test set[31] deals specifically with Diels−Alder reaction energies. It was found that even the local density approximation (SVWN functional) outperforms B3LYP (with mean absolute errors of 49.4 kJ mol^{-1} for SVWN and 64.5 kJ mol^{-1} for B3LYP, using def2-QZVP basis sets). While

Table 1. Comparison of DFT and Wave-Function Results for Gas-Phase Activation Barriers, $\Delta E^{\ddagger}$, and Reaction Energies, ΔE, in kJ mol^{-1} for Diels−Alder Reactions with Cyclopentadiene[a]

	MVK + CP		NQ + CP	
method and basis set	$\Delta E^{\ddagger}$	ΔE	$\Delta E^{\ddagger}$	ΔE
HF/CBS[b]	162.4	−52.5	167.1	−31.5
MP2/aug-cc-pVTZ	−24.9	−172.8	−57.2	−166.5
MP2/CBS[b]	−6.3	−160.2	−33.2	−150.0
SCS-MP2/aug-cc-pVTZ	13.1	−154.2	−12.2	−145.6
SCS-MP2/CBS[b]	33.5	−141.2	13.7	−128.8
CCSD/aug-cc-pVTZ	46.6	−149.1		
CCSD(T)/aug-cc-pVTZ	19.5	−152.3		
PBE0/def2-TZVP	46.9	−115.9	46.7	−92.7
PBE0-D3/def2-TZVP	27.4	−132.6	20.1	−114.5
B3LYP/def2-TZVP	78.1	−49.5	85.8	−24.5
B3LYP-D3/def2-TZVP	48.4	−75.6	46.5	−57.8
RIBP86/def2-TZVP	45.6	−71.1	52.3	−44.7
RIBP86-D3/def2-TZVP	10.6	−101.5	5.8	−83.9

[a]PBE0-D3/def2-TZVP gas-phase structures were used for the single-point wave function calculations. Fully optimized DFT/def2-TZVP and DFT-D3/def2-TZVP gas-phase results are shown for comparison. [b]Complete basis-set estimates for HF, MP2, and SCS-MP2 from two-point extrapolations of aug-cc-pVQZ and aug-cc-pV5Z data (see Table S1 in Supporting Information for complete data).

dx.doi.org/10.1021/ct5008857 | J. Chem. Theory Comput. XXXX, XXX, XXX−XXX

dispersion corrections reduce both barriers and reaction energies (Table 1) and thus improve agreement with the benchmark data, the B3LYP-D3 barriers are still overestimated by about 10−15 kJ mol^{-1} and, more notably, the reaction energies are too large by about 55−60 kJ mol^{-1}. This is likely related to the poor description of medium-range correlation effects by the B3LYP functional, which has been noted also for other organic reaction energies, for example, for rearrangements of hydrocarbons[32] or protobranching ratios[33,34] (the transition-state energies may actually benefit from some error compensation between different types of deficiencies for correlation effects). Notably, in the bimolecular reactions studied here, the errors are likely larger in the transition states and particularly in the products than in the separated reactants (including the dispersion contributions). The B3LYP hybrid functional overestimates the barriers and particularly underestimates the exothermicity of the two reactions. The "pure" gradient-corrected BP86 functional performs significantly better for the reaction energies than B3LYP: after inclusion of dispersion corrections, it seems that this functional underestimates the reaction energies by about 30 kJ mol^{-1} (the barriers are underestimated by about 20−25 kJ mol^{-1}). Overall, dispersion corrections reduce both activation barriers and reaction energies for all three functionals. While this generally improves the reaction energies, the barriers are in some cases deteriorated, in particular for BP86.

Compared to the benchmark data, the PBE0 functional provides the by far best reaction energies of the three functionals studied and, after inclusion of dispersion corrections, also excellent barriers. PBE0-D3 dispersion corrections are somewhat smaller than those for the other two functionals, likely reflecting a somewhat more attractive exchange-correlation potential provided by PBE0 itself. Its good agreement with the SCS-MP2/CBS and estimated CCSD(T)/CBS data makes the PBE0-D3 approach clearly suitable for our subsequent examination of solvent effects (possibly with errors in the barriers of up to about 10 kJ/mol and slightly larger deviations for the reaction energies; Table 1). This is in line with the much better performance of PBE0-D3 compared to B3LYP or B3LYP-D3 for the DARC Diels−Alder reaction energy and BHPERI[35−39] pericyclic reaction barrier test sets (previous B3LYP results with smaller basis sets sometimes gave the right answer for the wrong reason; see also Table S2 in Supporting Information for some PBE0 results with smaller basis sets and Supporting Information Tables S3 and S4 for comparisons of the three functionals with solvent models). While other functionals have been identified previously to also provide reasonable barriers and thermochemistry of DA reactions,[30] the PBE0-D3 approach has the advantage of being available in the TURBOMOLE 6.3 program package that we will use to evaluate the performance of COSMO and D-COSMO-RS solvent models (see below). Use of different structures for the post-HF single-point calculations does not appreciably alter the benchmark energetics nor the conclusions on the performance of DFT functionals (cf., Table S5 in Supporting Information).

Our evaluations so far have concentrated on the energetics. We note that dispersion corrections alter the structures of reactants, transition states and products relatively little. At PBE0-D3 level, changes in the important interatomic distances of the transition states because of dispersion (i.e., compared to PBE0) were less than 1% (see Figure 2 for the bond lengths in question). A slight reduction of the longer distance d_2 in the highly unsymmetrical transition state of the MVK + CP reaction by 2.1 pm was the largest structural change observed.

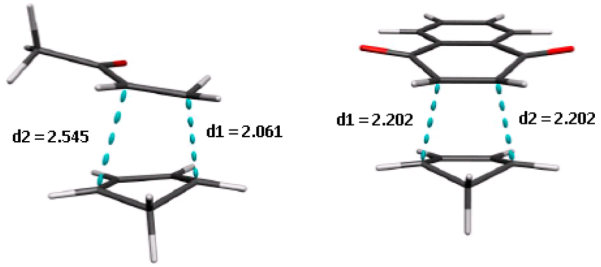

Figure 2. Definition of important interatomic distances of the transition states for the MVK + CP and NQ + CP reactions. PBE0-D3/def2-TZVP optimized distances in Å.

B. Modeling (Aqueous) Solvent Effects. The nature of the solvent may have a large impact on the kinetics (and partly the thermochemistry) of Diels−Alder cycloadditions. It is well-known that protic solvents like water and alcohols may lower reaction barriers by forming hydrogen bonds with polar groups.[40−42] For the two DA reactions studied here, these are largely the ketone/quinone oxygen atoms of MVK and 1−4-naphthoquinone, respectively. The hydrogen bonds are known to polarize the C═O bonds, which in turn affects the MO coefficients also throughout the entire dienophile and thereby stabilizes the transition state.[43−45] Our concentration will be on the solvent water. It is important in its own right, it is the most polar solvent used here (ε = 78.3553), and it is moreover expected to exhibit maximal effects of hydrogen bonding. Here we will, in addition to COSMO and D-COSMO-RS, also evaluate explicit inclusion of two water molecules hydrogen-bonded to a given ketone oxygen atom (i.e., overall two molecules for the MVK reaction and four molecules for the naphthoquinone reaction; see Figure 3) in

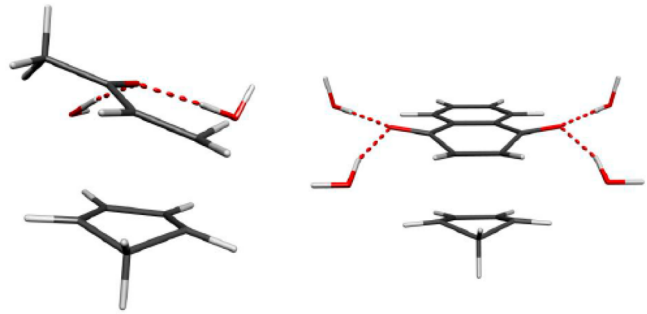

Figure 3. Transition states of the reactions of MVK and 1,4-naphthoquinone, respectively, with cyclopentadiene, including additional water molecules. PBE0-D3/def2-TZVP optimized structures.

static cluster models. For COSMO and D-COSMO-RS, we will in addition evaluate also methanol (ε = 32.613) as another protic solvent, as well as acetonitrile as polar aprotic solvent of similar dielectric constant (ε = 35.688), and hexane as apolar aprotic solvent (ε = 1.8819).

Thermochemical Considerations. Tables 2 and 3 summarize energies and Gibbs free energies of activation and reaction for the two title reactions, at various levels of treating the solvent effects. Dispersion effects turned out to substantially influence the energetics of the gas-phase reaction (see above). The two tables thus include data both with and without dispersion corrections in solution. Because of the partial

dx.doi.org/10.1021/ct5008857 | J. Chem. Theory Comput. XXXX, XXX, XXX−XXX

Table 2. Calculated Activation and Reaction Energies, Enthalpies and Gibbs Free Energies (in kJ mol^{-1}) for the MVK + CP Diels–Alder Reaction in Different Environments[a]

	$\Delta E^{\ddagger}$	$\Delta H^{\ddagger}_{298K}$	$\Delta G^{\ddagger}_{298K}$	ΔE	ΔH_{298K}	ΔG_{298K}
gas phase	46.9	47.6	100.3	−115.8	−104.0	−44.7
gas phase + D3	27.4	32.2	89.2	−132.6	−116.9	−54.8
gas phase + $2H_2O$	27.0	31.1	94.2	−116.1	−101.6	−40.0
gas phase + $2H_2O$ + D3	0.4	6.0	70.9	−136.1	−120.3	−57.6
COSMO-water	44.3	46.9	101.2	−109.9	−96.6	−37.2
COSMO-water + D3	28.9	34.1	91.4	−122.9	−107.1	−44.6
D-COSMO-RS-water	29.4	31.7	85.8	−115.4	−102.1	−42.9
D-COSMO-RS-water + D3	15.4	18.8	70.2	−128.7	−114.3	−54.7
COSMO-water + $2H_2O$	38.3	42.5	98.8	−105.2	−90.4	−28.6
COSMO-water + $2H_2O$ + D3	14.0	19.6	79.6	−129.3	−112.6	−39.9
D-COSMO-RS-water + $2H_2O$	30.4	37.1	94.5	−110.0	−91.6	−31.9
D-COSMO-RS-water + $2H_2O$ + D3	6.9	14.3	70.7	−129.2	−113.3	−44.5
Exp. (water)		**39.4**[b]	**80.4**			
COSMO-methanol	44.4	47.0	100.9	−110.2	−96.9	−37.4
COSMO-methanol + D3	25.0	27.9	82.5	−127.2	−113.7	−53.8
D-COSMO-RS-methanol	39.9	42.7	97.8	−109.4	−95.8	−35.7
D-COSMO-RS-methanol + D3	20.3	23.2	78.6	−126.3	−112.6	−52.4
Exp. 1-propanol (ethanol)		**45.1**[b]	**90.3 (90.5)**			
COSMO-acetonitrile	44.4	47.0	101.0	−110.1	−96.9	−37.5
COSMO-acetonitrile + D3	24.9	27.8	82.8	−127.2	−113.6	−53.8
D-COSMO-RS-acetonitrile	49.5	52.0	105.5	−106.5	−93.0	−33.8
D-COSMO-RS-acetonitrile + D3	30.1	32.9	86.7	−123.5	−109.8	−49.5
Exp. (acetonitrile)			**94.4**			
COSMO-hexane	48.0	50.9	104.3	−112.4	−98.6	−39.1
COSMO-hexane + D3	28.6	31.8	85.7	−129.2	−115.2	−55.9
D-COSMO-RS-hexane	55.5	58.4	111.5	−103.2	−89.5	−29.9
D-COSMO-RS-hexane + D3	36.2	39.4	92.9	−119.9	−106.1	−46.8

[a]PBE0/def2-TZVP results with and without D3 dispersion corrections. See Computational Details for evaluation of enthalpies and Gibbs free energies. Experimental data from ref 40 and 41. [b]From pseudothermodynamic analysis.

inclusion of dispersion between solute and solvent in the implicit solvent models (COSMO and D-COSMO-RS), it is of interest to first evaluate explicit (D3) dispersion effects on the energetics in the different environments to be able to decide which data are to be preferred in the analysis. Starting with the MVK + CP reaction (Table 2), the reduction due to dispersion (D3) of $\Delta E^{\ddagger}$ by 19.5 kJ/mol and of ΔE by 16.7 kJ/mol in the gas phase is affected almost negligibly for a COSMO treatment of the aprotic solvents hexane and acetonitrile, as well as for the D-COSMO-RS treatment of all solvents except water. COSMO-water reduces the dispersion contributions slightly to −15.4 and −13.0 kJ/mol, respectively. COSMO-methanol gives −15.4 and −17.0 kJ/mol, respectively. D-COSMO-RS-water leaves the overall smallest D3 contributions of −14.0 and −13.3 kJ/mol, respectively. That is, in the absence of explicit solvent molecules, the maximum effect of the implicit solvent (in this case D-COSMO-RS-water) on the D3 contributions is −5.5 kJ/mol for $\Delta E^{\ddagger}$ and −3.5 kJ/mol for ΔE, compared to the gas-phase dispersion contributions. This corresponds to almost additive behavior between D3 corrections and implicit solvent models. In contrast, the presence of two explicit water molecules enhances the D3 contributions to −26.6 and −20.0 kJ/mol, respectively, in the gas phase. This is modified to −24.3 kJ/mol and −24.1 kJ/mol, respectively, for COSMO-water + $2H_2O$ and to −23.5 and −19.2 kJ/mol, respectively, for D-COSMO-RS-water + $2H_2O$. An even clearer trend emerges for the 1,4-naphthoquinone + cyclopentadiene reaction (Table 3): in the gas phase and in any implicit solvent model (for any of the solvents studied), D3 corrections to $\Delta E^{\ddagger}$ are between −26.5 and −27.3 kJ/mol, and those to ΔE remain also almost constant between −21.8 kJ/mol and −22.6 kJ/mol. In contrast, inclusion of four explicit water molecules enhances the D3 contributions to $\Delta E^{\ddagger}$ to about −33 kJ/mol and those to ΔE to between −26 and −28 kJ/mol. It is thus clear that the explicit dispersion corrections to both energies become more negative for both reactions, when explicit water molecules are present, whereas differences between the various implicit solvent treatments remain small. This has to be kept in mind when evaluating the solvent effects computed with explicit vs implicit solvent modeling.

As discussed above, computed entropic contributions to the Gibbs free activation and reaction energies arise only from internal degrees of freedom, whereas the experimental estimates contain to some degree solvent contributions as well. We should therefore not attempt to directly compare the entropy contributions (and thus the exclusively enthalpic contributions) with experiment. Yet we may compare the different models. Starting with the entropic contributions to $\Delta G^{\ddagger}_{298K}$ of the MVK + CP reaction (difference between $\Delta G^{\ddagger}_{298K}$ and $\Delta H^{\ddagger}_{298K}$), we see in Table 2 that the implicit solvent model data vary only between +51 and +58 kJ/mol. Dispersion contributions influence these values by less than 5 kJ/mol. Addition of explicit water molecules in cluster models increases the entropic contributions only slightly. In fact the variations found are probably within the numerical noise caused by numerical differentiation of analytical gradients in the vibrational analyses. The entropic contributions to the Gibbs free reaction energies (ΔG_{298K}) vary over an even narrower range,

dx.doi.org/10.1021/ct5008857 | J. Chem. Theory Comput. XXXX, XXX, XXX−XXX

Table 3. Calculated Activation and Reaction Energies, Enthalpies, and Gibbs Free Energies (in kJ mol^{-1}) NQ + CP Diels–Alder Reaction in Different Environments[a]

	$\Delta E^{\ddagger}$	$\Delta H^{\ddagger}_{298K}$	$\Delta G^{\ddagger}_{298K}$	ΔE	ΔH_{298K}	ΔG_{298K}
gas phase	46.7	49.7	108.5	−92.7	−79.7	−19.3
gas phase + D3	20.1	24.5	84.2	−114.5	−100.1	−38.8
gas phase + 4H_2O	17.8	21.6	85.4	−100.2	−86.7	−23.6
gas phase + 4H_2O + D3	−15.7	−10.6	53.3	−128.1	−112.9	−46.0
COSMO-water	42.2	45.3	103.9	−86.1	−73.1	−12.4
COSMO-water + D3	15.5	20.0	79.6	−108.5	−94.1	−32.3
D-COSMO-RS-water	25.4	28.6	86.9	−95.5	−82.4	−21.2
D-COSMO-RS-water + D3	−1.9	1.5	60.4	−118.1	−104.6	−42.8
COSMO-water + 4H_2O	32.5	(34.0[c])	(98.0[c])	−92.0	(−78.0[c])	(−14.0[c])
COSMO-water + 4H_2O + D3	0.3	2.0	65.6	−118.2	−103.4	−39.8
D-COSMO-RS-water + 4H_2O	29.1	(30.5[c])	(94.5[c])	−94.2	(−80.0[c])	(−16.0[c])
D-COSMO-RS-water + 4H_2O + D3	−3.3	(−1.5[c])	(62.5[c])	−120.4	(−105.5[c])	(−41.5[c])
exp. (water)		**36.6**[b]	**69.4**			
COSMO-methanol	42.5	45.6	104.2	−86.3	−73.2	−12.6
COSMO-methanol + D3	15.8	18.9	77.7	−108.7	−95.3	−33.6
D-COSMO-RS-methanol	43.1	45.4	103.5	−83.7	−70.9	−10.4
D-COSMO-RS-methanol + D3	16.3	19.0	78.0	−106.0	−92.9	−31.5
exp. (1-propanol)		**42.9**[b]	**83.1**			
COSMO-acetonitrile	42.4	45.6	104.2	−86.3	−73.2	−12.5
COSMO-acetonitrile + D3	15.8	19.2	78.5	−108.7	−95.2	−33.7
D-COSMO-RS-acetonitrile	49.2	52.1	110.7	−80.2	−67.2	−6.6
D-COSMO-RS-acetonitrile + D3	22.6	25.8	84.8	−102.5	−89.2	−28.3
exp. (acetonitrile)			**86.2**			
COSMO-hexane	45.8	48.9	107.6	−90.3	−77.2	−16.0
COSMO-hexane + D3	19.2	22.6	81.8	−112.3	−99.0	−38.2
D-COSMO-RS-hexane	54.0	57.1	115.5	−81.0	−68.1	−7.1
D-COSMO-RS-hexane + D3	27.5	31.0	90.3	−103.0	−89.7	−28.6
exp. (hexane)			**90.4**			

[a]PBE0/def2-TZVP results with and without D3 dispersion corrections. See Computational Details for evaluation of enthalpies and Gibbs free energies. Experimental data from ref 40. [b]From pseudothermodynamic analysis. [c]Due to spurious imaginary frequencies, the entropic and thermal contributions were estimated by analogy to closely related calculations.

from +59 to +63 kJ/mol (Table 2). These values are close to the activation entropy contributions, in keeping with a late transition state of a bimolecular reaction, where the new bonds have already been formed to a great extent. Turning to the NQ + CP reaction, results are very similar, with computed entropic activation contributions between +58 and +64 kJ/mol and contributions to the reaction energies between +60 and +67 kJ/mol. Here three models with embedded water molecules gave spurious imaginary H_2O vibrational frequencies (see Computational Details and Table 3). Thus, the corresponding entropic and thermal contributions are only estimates (albeit reasonable ones).

With these considerations in mind, we compare now the performance of the different solvent models overall. Our main focus is on the effect of aqueous solvent, and we thus start our discussion with the pertinent data. When trying to establish a benchmark level for aqueous solvent effects on the energetics, against which D-COSMO-RS-water may be compared, we note that addition of explicit hydrogen-bonded water molecules in the gas phase is expected to overestimate the overall solvent effects, as the added H_2O molecules lack an embedding into the bulk. Indeed, embedding the explicitly solvated cluster models into a COSMO-water environment reduces the overall effects on both $\Delta E^{\ddagger}$ and ΔE (and thus on $\Delta G^{\ddagger}_{298K}$ and on ΔG_{298K}) compared to the clusters in vacuum (Tables 2 and 3). These embedded clusters appear a reasonable starting point for the evaluation of D-COSMO-RS-water, keeping in mind the above-mentioned differences in the D3 dispersion for explicit vs implicit solvation.

However, we have to account for the fact that semiempirical QM/MM molecular dynamics simulations on both reactions by Acevedo and Jorgensen[46] provided solute–solvent radial distribution functions more consistent with an average of three hydrogen bonds per keto oxygen atom, in particular for the transition state, and more pronouncedly so for the MVK + CP than for the NQ + CP reaction. While the quantitative accuracy of the QM/MM simulations is limited by the semiempirical PDDG/PM3 method used for the QM part (e.g., the method underestimates significantly the transition-state asymmetry for the gas-phase MVK+CP reaction compared to CBS-QB3 data, and free activation energies tend to be overestimated by up to 65 kJ/mol[46]), qualitatively the increase of hydrogen bonding interactions at the transition state is convincing. We have thus attempted to also optimize static cluster models with three water molecules for MVK and with six water molecules for NQ. However, these optimizations did not lead to usable minima or transition states. In case of the NQ + CP reaction, during optimization the third water molecule generally dissociated from the quinone oxygen atom and formed hydrogen bonds with one of the other water molecules present. For the transition state of the MVK + CP reaction, structures with three water molecules hydrogen-bonded to the keto oxygen atom could indeed be obtained. However, these structures nevertheless revealed hydrogen

dx.doi.org/10.1021/ct5008857 | J. Chem. Theory Comput. XXXX, XXX, XXX–XXX

bonds *between* the water molecules. This suggests that the energetics obtained with these structures would not faithfully represent the average situation in aqueous solution, where the most unstrained hydrogen bonds likely are with further surrounding water molecules. It appears likely, nevertheless, that the true average situation in aqueous solution would be somewhere between 2 and 3 hydrogen bonds per keto oxygen atom at the transition states, with the MVK-CP systems favoring stronger interactions than the NQ + CP system.

We first compare directly the D-COSMO-RS results with experiment, focusing on Gibbs free energies rather than enthalpies, due to the above-mentioned difficulties of separating the solvent entropic from enthalpic contributions for implicit solvent models. In case of the MVK + CP reaction, for the three solvents for which experimental gibbs free activation energies are available, the PBE0/D-COSMO-RS data without D3 corrections tend to overestimate the experimental $\Delta G^{\ddagger}_{298K}$ values by ~14 kJ/mol for water, by ~8 kJ/mol for methanol (experimental data for 1-propanol or ethanol are almost identical), and by ~9 kJ/mol for acetonitrile. Adding D3 corrections provides a remarkably consistent *underestimate* by 8−10 kJ/mol instead. This underestimate may well reflect the intrinsic error of the PBE0+D3/def2-TZVP approach (see above and Table 1), so that we conclude the D-COSMO-RS results at this level to provide systematically good agreement with experimental $\Delta G^{\ddagger}_{298K}$ values for the different solvents.

This may be appreciated better when we concentrate on relative Gibbs free activation energies for different solvents, as has been done previously for both title reactions by Acevedo and Jorgensen using their semiempirical PDDG/PM3/MM/MC approach.[46] Figures 4 and 5 provide this type of comparison of the pure relative solvent effects for the MVK + CP and NQ + CP reactions, respectively. We show the values relative to acetonitrile solvent, as the more natural reference point with the nonpolar solvent hexane has so far not been

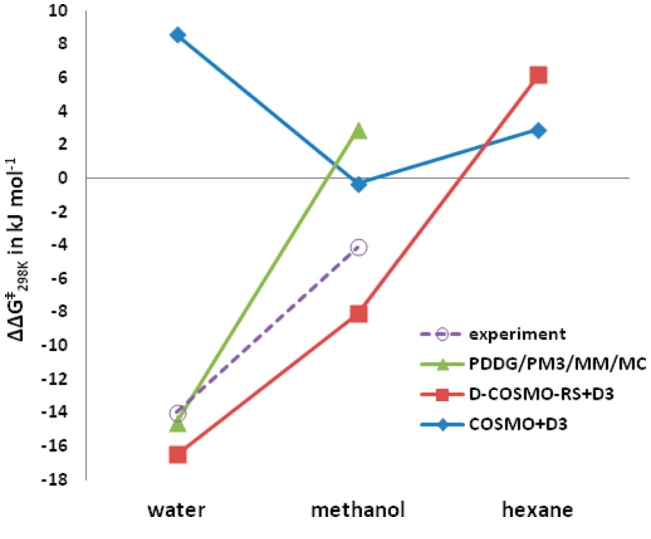

Figure 4. Solvent contributions to the Gibbs free activation energy of the MVK + CP reaction relative to acetonitrile using different methods. The semiempirical PDDG/PM3/MM/MC calculations are from ref 46. The present calculations are provided at PBE0/def2-TZVP+D3 level (see Figure S1 in Supporting Information for corresponding results without dispersion corrections). Experimental data from ref 42.

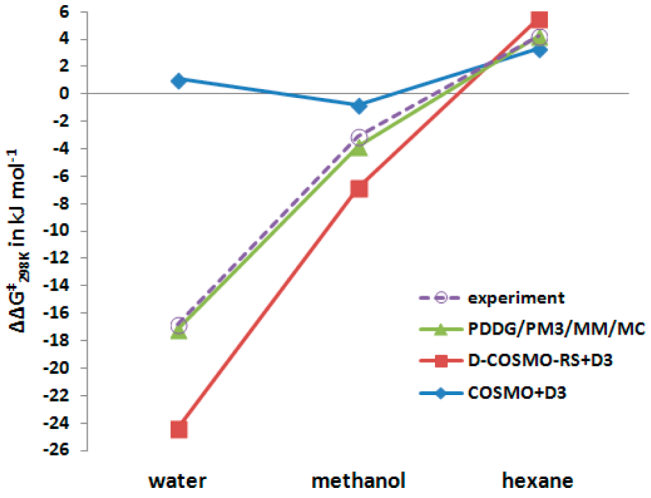

Figure 5. Solvent contribution to the Gibbs free activation energy of the NQ + CP reaction relative to acetonitrile using different methods. The semiempirical PDDG/PM3/MM/MC calculations are from ref 46. The present calculations are provided at PBE0/def2-TZVP+D3 level (see Figure S2 in Supporting Information for corresponding results without dispersion corrections). Experimental data from ref 42.

studied experimentally for the MVK + CP reaction (the corresponding point lacks therefore in Figure 4).

The negative experimental values for the protic solvents show clearly the reduction of the Gibbs free-energy barrier relative to acetonitrile, while the positive hexane value for the NQ + CP reaction is consistent with the lower polarity of hexane compared to acetonitrile. The previous PDDG/PM3/MM/MC results reproduce the experimental differences excellently for the NQ + CP reaction, in spite of the rather large errors in the absolute Gibbs free activation energies at this computational level (see above). An incorrect positive value for methanol is obtained for the MVK + CP reaction, for unclear reasons.

COSMO provides clearly very poor relative values. One might have expected small negative values for water, due to its larger dielectric constant compared to acetonitrile. However, an appreciably positive value is obtained for the MVK + CP reaction (Figure 4), and a small positive one for the NQ + CP reaction (Figure 5). The positive values seem to be an artifact of the combination of COSMO with the D3 dispersion corrections: Figures S1 and S2 in Supporting Information show that without dispersion contributions the expected small COSMO values for water are obtained.

D-COSMO-RS seems to be affected less by this problem: for the MVK + CP reaction, dispersion contributions reduce the difference between methanol and water slightly (Figure 4 and Supporting Information Figure S1), but for NQ+CP the curves with and without dispersion are very similar (Figure 5 and Supporting Information Figure S2). While overall somewhat too large reductions of the Gibbs free-energy barriers by the protic solvents are found compared to experiment, the trends are reproduced rather well for both reactions, in sharp contradiction to the COSMO data, but in relatively good agreement with the previous semiempirical MC data.

Turning to the comparison of D-COSMO-RS-water data with the cluster-model results for the MVK+CP reaction (Table 2), we see that without D3 corrections, D-COSMO-RS provides 13 kJ/mol lower $\Delta G^{\ddagger}_{298K}$ than the embedded-cluster model (COSMO-water + $2H_2O$). After inclusion of D3

dx.doi.org/10.1021/ct5008857 | J. Chem. Theory Comput. XXXX, XXX, XXX−XXX

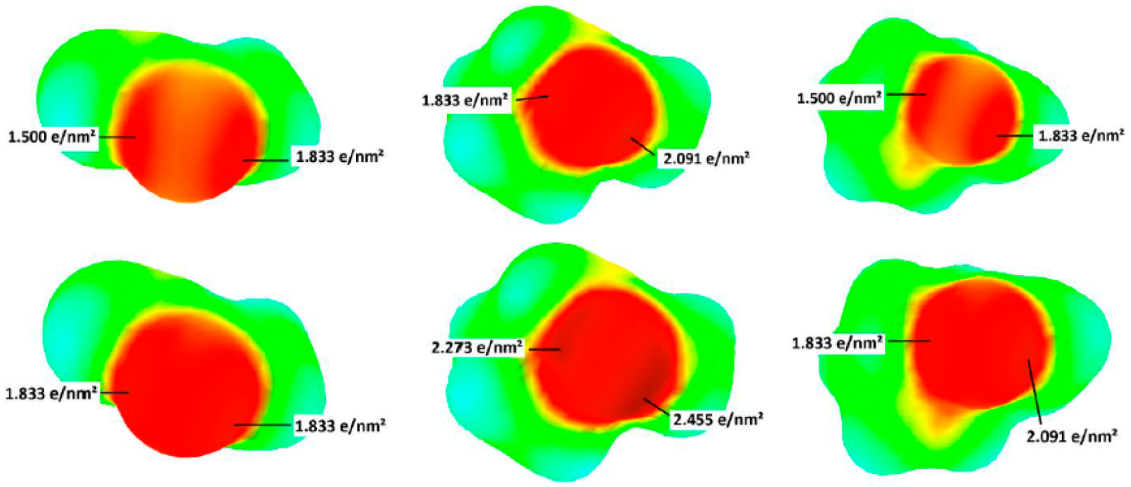

Figure 6. Surface charge density maps for the MVK + CP reaction. The upper row from left to right shows reactant (MVK), transition state and product, respectively, with COSMO (water). The lower row from left to right shows reactant, transition state, and product, respectively, with D-COSMO-RS (water).

corrections, the difference shrinks to about 9 kJ/mol. For the Gibbs free reaction energies (ΔG_{298K}), we see that the D-COSMO-RS-water value is about 14 kJ/mol more exothermic than COSMO-water+2H_2O. Here the difference remains essentially constant upon inclusion of D3 corrections. These results suggest that D-COSMO-RS-water simulates a situation with somewhat more differential hydrogen-bonding interactions than provided by the COSMO-water + 2H_2O embedded-cluster models, regarding both the Gibbs free activation energy (more H-bonding in the transition state than in the reactants) and the Gibbs free reaction energy (more H-bonding in the product than in the reactants). This result would be consistent with the situation described by the previous QM/MM MC studies,[46] where more than an average number of two hydrogen bonds were found for the transition state and the product (see above). In contrast to the Gibbs free activation energy, we have no experimental value for the Gibbs free reaction energy to compare with. Combining the D-COSMO-RS-water approach with two explicit water molecules provides somewhat less consistent results. While the two added water molecules render the reactions about 10 kJ/mol less endergonic, independent of the presence or absence of the D3 corrections, the effect on the Gibbs free activation energies depends on the dispersion terms (increased $\Delta G^{\ddagger}_{298K}$ without dispersion, an almost constant value with D3 correction). Overall, use of D-COSMO-RS-water without added explicit water molecules appears to be preferable.

Turning to the NQ + CP reaction (Table 3) we find again that PBE0+D3/def2-TZVP with D-COSMO-RS-water provides a ∼9 kJ/mol too low $\Delta G^{\ddagger}_{298K}$ value compared to experiment, similar to the results for MVK + CP above (Table 2). The underestimate of the Gibbs free activation energy at PBE0+D3/def2-TZVP/D-COSMO-RS level is smaller for the other solvents (∼6 kJ/mol for alcohols, ∼1−2 kJ/mol for acetonitrile, essentially zero for hexane). Without D3 corrections, the Gibbs free activation energies are overestimated more clearly (by ∼17 kJ/mol for water, by ∼20 kJ/mol for alcohol, by ∼14−15 kJ/mol for acetonitrile, and by ∼25 kJ/mol for hexane). That is, the MVK + CP and NQ + CP results together are not sufficiently systematic to attribute beyond doubt the underestimate of the Gibbs free activation energies for most cases to the underlying PBE0+D3/def2-TZVP level.

Comparison of the D-COSMO-RS-water data with the embedded-cluster models for the NQ + CP reaction (Table 3) gives a somewhat different picture than discussed above (Table 2) for the MVK + CP reaction: now D-COSMO-RS-water is much closer to the embedded-cluster data (COSMO-water + 4H_2O), both with and without D3 corrections, and for both Gibbs free activation and reaction energies. Differences are generally below 5 kJ/mol (note the only estimated entropy contributions, see above). This is in keeping with the notion (based on QM/MM MD data[46]) of somewhat weaker and longer hydrogen bonds for a given keto oxygen atom in the NQ + CP reaction. Two hydrogen bonds per keto (here: quinone) oxygen atom appears to be a better average description for NQ + CP than for MVK + CP, even for the transition state and the product. Again, experimental data for the Gibbs free reaction energies are lacking. We may take the approximately −40 kJ/mol obtained both with D-COSMO-RS-water + D3 and with COSMO-RS-water + 4H_2O + D3 as reasonable estimate (within the limits of accuracy of the underlying PBE0+D3/def2-TZVP level). We note in passing that D-COSMO-RS-water + 4H_2O + D3 provides an unrealistically low Gibbs free activation energy, consistent with the discussion above, which disfavored the use of explicit water molecules together with the D-COSMO-RS-water model.

On the other hand, it is obvious and in agreement with previous work[46] that, for both reactions studied here, a polarizable continuum model without explicit water molecules cannot provide the observed, appreciable lowering of the Gibbs free activation energies in aqueous solution (Figures 4 and 5). The effects on the Gibbs free reaction energies are smaller. Yet the errors of a COSMO treatment may also exceed already the accuracy limitations provided by the underlying electronic-structure method. In the absence of reliable experimental data we may judge this only indirectly from the good performance of PBE0+D3/def2-TZVP for the gas-phase reaction energy (cf., Table 1). For methanol, the second protic solvent studied here, COSMO reproduces the D-COSMO-RS data better, both for activation and reaction energies (Tables 2 and 3). While this seems surprising at first, it might reflect the somewhat smaller hydrogen bonding effects in alcoholic solutions.

For the aprotic solvents one expects little differences between COSMO and D-COSMO-RS. This holds indeed for acetoni-

dx.doi.org/10.1021/ct5008857 | J. Chem. Theory Comput. XXXX, XXX, XXX−XXX

trile, where the COSMO and D-COSMO-RS data agree within less than 5 kJ/mol (for both $\Delta G^{\ddagger}_{298K}$ and ΔG_{298K}; Tables 2 and 3). Note, however, that the D-COSMO-RS data are systematically more positive by this amount. Maximal differences between COSMO and D-COSMO-RS increase to about 10 kJ/mol for hexane, with D-COSMO-RS again systematically providing more positive Gibbs free activation and reaction energies (see also Figures 4 and5). This is similar to observations made for electron-transfer barriers in organic mixed-valence systems.[7,36]

Interpretation of Solvent Effects in Terms of Electronic Structure. The above results suggest that the D-COSMO-RS surface charge densities may implicitly incorporate different effective numbers or spatial extent of hydrogen-bonding hotspots. To evaluate how this functions in practice, we have graphically and numerically analyzed these surface charge densities. For the MVK reactant and the MVK + CP transition state and product, plots of surface charge densities obtained after the self-consistent COSMO-water and D-COSMO-RS-water calculations are shown in Figure 6 (further plots are given in Figures S3 and S4 in Supporting Information). It is clear that the surface charge polarization around the keto oxygen atom is a) significantly enhanced at D-COSMO-RS compared to COSMO level, and b) the polarization is substantially more pronounced at the transition state compared to reactant or product, again in particular for D-COSMO-RS. At the transition state, enhanced D-COSMO-RS surface charge densities cover a much larger area around the oxygen atom. This is consistent both with stronger hydrogen bonding and with a larger average number of contacts. We note that the largest surface charge densities are not distributed in a cylindrical arrangement but show a distinct accumulation away from the more sterically hindered parts of the transition-state structure. The polarization for the NQ + CP transition state (Supporting Information Figure S3) is also enhanced significantly compared to the NQ reactant (or the product). However, it is appreciably less pronounced compared to the MVK + CP transition state (Figure 6). This likely reflects less effective hydrogen bonding in the NQ + CP transition state, consistent with our inability to optimize static model clusters with three water molecules hydrogen-bonded to each of the quinone oxygen atoms (see above). Similarly, the D-COSMO-RS surface charge densities of reactant and product of the NQ + CP reaction also feature less pronounced maxima than for MVK + CP (Figure 6, Supporting Information Figure S3). We thus conclude that D-COSMO-RS surface charge densities apparently reflect differences not only between the intensity of average hydrogen-bonding contacts at the transition states compared to reactants or products but also differences between the two reactions studied here. This is notable in view of the fact that the D-COSMO-RS-water energetics of the NQ + CP agree well with the COSMO-water + $4H_2O$ static cluster model results (cf., Table 3), whereas they provide a larger reduction of Gibbs free activation energy than COSMO-water + $2H_2O$ data for the MVK + CP reaction (cf., Table 2).

The environmental effects on electronic structure may be evaluated additionally from partial atomic charges, in particular for the oxygen atoms that may act as acceptors for hydrogen bonding. Table 4 provides oxygen NPA charges for reactant, transition state, as well as product of the MVK + CP reaction, using different solvent environments. We note in passing that dispersion contributions influence these charges only indirectly by structural modifications. First of all, the oxygen charges of reactant and product differ relatively little, while they are distinctly more negative at the transition state, consistent with previous analyses.[44,46,47] This explains why protic solvents have a much larger lowering effect on the activation barriers than on the reaction energies (see above). The charges are generally rendered more negative by polar solvents, and the changes due to solvent are also largest at the transition state. Let us focus on aqueous solution: most notably, the enhancement of the charges (compared to the gas-phase values) is largest for D-COSMO-RS-water, somewhat less pronounced for COSMO-water + $2H_2O$, and still much less for COSMO-water without explicit solvent molecules. This confirms that (a) the COSMO continuum solvent does not capture the hydrogen-bonding effects adequately and (b) D-COSMO-RS seems to provide a stronger hydrogen-bonding environment than the COSMO-water + $2H_2O$ embedded-cluster model, consistent with the larger average number of hydrogen bonds obtained in MD simulations.[45,46] And as the overall effects are largest at the transition state (charges relative to the gas-phase values −0.14 for reactant, −0.16 for the transition state, and −0.13 for the product, Table 4), the appreciable lowering of the activation barrier with D-COSMO-RS-water is easily understood. We furthermore note also that addition of explicit water molecules to D-COSMO-RS-water has almost no additional effect on the

Table 4. Important Distances (in Å) in the Transition State and Natural Charges on the Ketone Oxygen Atom for the MVK + Cyclopentadiene Diels−Alder Reaction in Different Environments[a]

	d_1	d_2	q_{educt}	q_{trans}	$q_{product}$
gas phase	2.064	2.566	−0.52	−0.58	−0.53
gas phase + D3	2.061	2.545	−0.52	−0.58	−0.53
gas phase + $2H_2O$	2.058	2.739	−0.60	−0.69	−0.61
gas phase + $2H_2O$ + D3	2.054	2.711	−0.60	−0.69	−0.61
COSMO-water	2.055	2.634	−0.60	−0.67	−0.60
COSMO-water + D3	2.056	2.607	−0.59	−0.67	−0.60
D-COSMO-RS-water	2.068	2.706	−0.67	−0.75	−0.66
D-COSMO-RS-water + D3	2.060	2.645	−0.66	−0.74	−0.66
COSMO-water + $2H_2O$	2.068	2.729	−0.63	−0.72	−0.64
COSMO-water + $2H_2O$ + D3	2.062	2.715	−0.63	−0.72	−0.63
D-COSMO-RS-water + $2H_2O$	2.064	2.730	−0.64	−0.73	−0.64
D-COSMO-RS-water + $2H_2O$ + D3	2.071	2.737	−0.64	−0.74	−0.64
COSMO-methanol	2.055	2.631	−0.59	−0.67	−0.60
COSMO-methanol + D3	2.055	2.611	−0.60	−0.67	−0.60
D-COSMO-RS-methanol	2.061	2.696	−0.60	−0.73	−0.60
D-COSMO-RS-methanol + D3	2.061	2.676	−0.60	−0.73	−0.60
COSMO-acetonitrile	2.055	2.631	−0.60	−0.67	−0.60
COSMO-acetonitrile + D3	2.054	2.603	−0.60	−0.67	−0.60
D-COSMO-RS-acetonitrile	2.054	2.609	−0.58	−0.64	−0.58
D-COSMO-RS-acetonitrile + D3	2.051	2.587	−0.58	−0.65	−0.58
COSMO-hexane	2.060	2.579	−0.54	−0.61	−0.55
COSMO-hexane + D3	2.057	2.561	−0.54	−0.61	−0.55
D-COSMO-RS-hexane	2.059	2.582	−0.55	−0.61	−0.56
D-COSMO-RS-hexane + D3	2.057	2.559	−0.55	−0.61	−0.56

[a]PBE0/def2-TZVP results with and without D3 dispersion corrections. See Figure 2 for definition of the distances.

dx.doi.org/10.1021/ct5008857 | J. Chem. Theory Comput. XXXX, XXX, XXX−XXX

oxygen charges. The interpretation of the oxygen atomic charges is thus fully consistent with the above analyses of the surface-charge density profiles.

Transition-State Structures. A main difference between the two title reactions is that for MVK + CP the transition state is very unsymmetrical (see d_1 vs d_2 in Table 4, Figure 2), whereas it is essentially symmetrical for the NQ+CP reaction (Table S6 in Supporting Information). This influences the magnitude of dispersion and solvent effects at the transition-state structures: the two almost equivalent C−C distances, d_1, d_2, of the latter reaction vary over an intermediate range of maximally 0.075 Å (Supporting Information Table S5), whereas in the former reaction, the long distance d_2 changes by up to 0.194 Å, the shorter d_1 only by maximally 0.020 Å. For the MVK + CP reaction, the asymmetry of the transition state is typically enhanced by solvent effects and decreased by dispersion (Table 4). This is mainly because of the changes in d_2: dispersion contracts the longer distance much more than d_1, by typically up to 0.03 Å (but by exceptional 0.06 Å for D-COSMO-RS-water). Solvent effects on d_2 are even more pronounced. They increase the distance by up to almost 0.2 Å at some levels (by 0.140/0.100 Å for D-COSMO-RS-water + D3). Here the solvent and dispersion effects are clearly nonadditive. For the NQ + CP reaction (Table S6 in Supporting Information), only D-COSMO-RS with very polar solvents introduces a slight asymmetry into the transition-state structure. And this might even be a small numerical artifact of the solvent treatment. Here we should thus evaluate the overall shortening or lengthening effects on the average of d_1 and d_2: dispersion shortens these intermediate distances typically only by up to 0.010 Å (0.015 Å for gas phase + $4H_2O$, whereas D-COSMO-RS + $4H_2O$ even exhibits a slight lengthening due to dispersion). Solvent effects on the two distances also remain small, except for D-COSMO-RS-water + $4H_2O$, where a lengthening by about 0.02−0.04 Å is found, depending on dispersion.

4. CONCLUSIONS

COSMO-RS is an implicit solvent model, which requires comparable computational effort and can be carried out essentially in the same black-box mode as standard polarizable dielectric continuum solvent models like COSMO. Nevertheless, the implicitly included hydrogen-bond terms make COSMO-RS much more suitable for protic solvents, in particular for aqueous solution, and it may be applied to solvent mixtures. While we should not expect a completely quantitative treatment of specific solvent contributions, COSMO-RS has clearly been shown in the past to offer great potential for many applications. These advantageous properties of COSMO-RS obviously carry over to its self-consistent variant, D-COSMO-RS, which allows computations of structures or vibrational frequencies. Its favorable performance in recent electron-transfer studies has been confirmed here for kinetics and thermochemistry of Diels−Alder reactions, and it is likely to hold for many other chemical reactions as well. Together with the possibility of computing further molecular properties, this opens many areas of application for this convenient solvent model. These findings are remarkable in view of the fact that COSMO-RS and D-COSMO-RS do not require MD or MC simulations. While QM/MM MC simulations had been carried out previously for the two title reactions of the present work, they had been limited to a rather approximate semiempirical MO method, due to the substantial effort involved in carrying out millions of QM calculations. In contrast, the much lower computational effort involved in D-COSMO-RS has allowed us to use much better underlying QM methods. Other methods, such as RISM-SCF, should of course be mentioned as interesting alternatives.

A useful feature of the present D-COSMO-RS simulations is the capture of fractional and variable average numbers of hydrogen bonds, which turned out to differ between reactants, transition states and products of the two reactions studied here. We furthermore observed slight numerical instabilities of vibrational frequency computations with COSMO, but particularly with D-COSMO-RS, as a moderate drawback of the current implementation, in particular for transition states and in the presence of explicit water molecules. This will require further evaluation.

As a basis for comparison with experimental Gibbs free energies of activation and reaction, it also turned out to be crucial to carefully choose the underlying electronic-structure method. Here we concentrated on the PBE0+D3/def2-TZVP level, which compared favorably with benchmark ab initio calculations in the gas phase. Other functionals are known to show comparable accuracy for pericyclic reactions, while the previously observed deficiencies of the B3LYP functional for certain types of organic reactions were clearly exposed in our evaluations. It is also important to reiterate that B3LYP calculations with small basis sets like 6-31G(d) may give the right answer for the wrong reason.

■ ASSOCIATED CONTENT

Ⓢ Supporting Information

Tables and figures with additional computational data. This material is available free of charge via the Internet at http://pubs.acs.org.

■ AUTHOR INFORMATION

Corresponding Author

*E-mail: martin.kaupp@tu-berlin.de.

Notes

The authors declare no competing financial interest.

■ ACKNOWLEDGMENTS

This work has been supported by DFG within Sonderforschungsbereich 1109 (Teilprojekt A03). Dr. Andreas Klamt (COSMOlogic GmbH, Leverkusen) is gratefully acknowledged for useful discussions.

■ REFERENCES

(1) *Continuum Solvation Models in Chemical Physics*; John Wiley & Sons, Ltd.: Chichester, U.K., 2007.

(2) Cossi, M.; Rega, N.; Soteras, I.; Blanco, D.; Huertas, O.; Bidon-Chanal, A.; Luque, F. J.; Truhlar, D. G.; Pliego, J. R.; Ladanyi, B. M.; Newton, M. D.; Domcke, W.; Sobolewski, A. L.; Laage, D.; Burghardt, I.; Hynes, J. T.; Persico, M.; Granucci, G.; Huxter, V. M.; Scholes, G. D.; Curutchet, C. *Continuum Solvation Models in Chemical Physics*; John Wiley & Sons, Ltd.: Chichester, U.K., 2007; Chapter 3, pp 313−498.

(3) Tomasi, J.; Cancès, E.; Pomelli, C. S.; Caricato, M.; Scalmani, G.; Frisch, M. J.; Cammi, R.; Basilevsky, M. V.; Chuev, G. N.; Mennucci, B. *Continuum Solvation Models in Chemical Physics*; John Wiley & Sons, Ltd.: Chichester, U.K., 2007; Chapter 1, pp 1−124.

(4) Klamt, A. *J. Phys. Chem.* **1995**, *99*, 2224.

(5) Eckert, F.; Klamt, A. *AIChE J.* **2002**, *48*, 369.

(6) Sinnecker, S.; Rajendran, A.; Klamt, A.; Diedenhofen, M.; Neese, F. *J. Phys. Chem. A* **2006**, *110*, 2235.

(7) Renz, M.; Kess, M.; Diedenhofen, M.; Klamt, A.; Kaupp, M. *J. Chem. Theory Comput.* **2012**, *8*, 4189.
(8) Dirac, P. A. M. *Proc. Cambridge Philos. Soc.* **1930**, *26*, 376.
(9) Slater, J. C. *Phys. Rev.* **1951**, *81*, 385.
(10) Perdew, J. P.; Wang, Y. *Phys. Rev. B* **1992**, *45*, 13244.
(11) Perdew, J. P.; Burke, K.; Ernzerhof, M. *Phys. Rev. Lett.* **1996**, *77*, 3865.
(12) Perdew, J. P.; Ernzerhof, M.; Burke, K. *J. Chem. Phys.* **1996**, *105*, 9982.
(13) Grimme, S.; Antony, J.; Ehrlich, S.; Krieg, H. *J. Chem. Phys.* **2010**, *132*, No. 154104.
(14) Ahlrichs, R.; Baer, M.; Haeser, M.; Horn, H.; Koelmel, C. *Chem. Phys. Lett.* **1989**, *162*, 165.
(15) Treutler, O.; Ahlrichs, R. *J. Chem. Phys.* **1995**, *102*, 346.
(16) TURBOMOLE V6.3, A development of University of Karlsruhe and Forschungszentrum Karlsruhe GmbH, 1989−2007; TURBOMOLE GmbH, 2007. http://www.turbomole.com (accessed Nov. 8, 2014).
(17) Weigend, F.; Ahlrichs, R. *Phys. Chem. Chem. Phys.* **2005**, *7*, 3297.
(18) Dunning, T. H. *J. Chem. Phys.* **1989**, *90*, 1007.
(19) Kendall, R. A.; Dunning, T. H.; Harrison, R. J. *J. Chem. Phys.* **1992**, *96*, 6796.
(20) Vosko, S. H.; Wilk, L.; Nusair, M. *Can. J. Phys.* **1980**, *58*, 1200.
(21) Becke, A. D. *Phys. Rev. A* **1988**, *38*, 3098.
(22) Lee, C.; Yang, W.; Parr, R. G. *Phys. Rev. B* **1988**, *37*, 785.
(23) Becke, A. D. *J. Chem. Phys.* **1993**, *98*, 5648.
(24) Perdew, J. P. *Phys. Rev. B* **1986**, *33*, 8822.
(25) Grimme, S. *J. Chem. Phys.* **2003**, *118*, 9095.
(26) Halkier, A.; Helgaker, T.; Jørgensen, P.; Klopper, W.; Koch, H.; Olsen, J.; Wilson, A. K. *Chem. Phys. Lett.* **1998**, *286*, 243.
(27) Eckert, F.; Klamt, A. *COSMOtherm*, version C2.1, release 01.11; COSMOlogic GmbH & Co. KG: Leverkusen, Germany, 2010.
(28) Orozco, M.; Marchán, I.; Soteras, I.; Vreven, T.; Morokuma, K.; Mikkelsen, K. V.; Milani, A.; Tommasini, M.; Zoppo, M. D.; Castiglioni, C.; Aguilar, M. A.; Sánchez, M. L.; Martín, M. E.; Galván, I. F.; Sato, H. *Continuum Solvation Models in Chemical Physics*; John Wiley & Sons, Ltd.: Chichester, U.K., 2007; Chapter 4, pp 499−606.
(29) Pieniazek, S. N.; Clemente, F. R.; Houk, K. N. *Angew. Chem., Int. Ed.* **2008**, *47*, 7746.
(30) Johnson, E. R.; Mori-Sánchez, P.; Cohen, A. J.; Yang, W. *J. Chem. Phys.* **2008**, *129*, No. 204112.
(31) Goerigk, L.; Grimme, S. *J. Chem. Theory Comput.* **2010**, *7*, 291.
(32) Grimme, S. *Angew. Chem., Int. Ed.* **2006**, *45*, 4460.
(33) Wodrich, M. D.; Wannere, C. S.; Mo, Y.; Jarowski, P. D.; Houk, K. N.; Schleyer, P. v. R. *Chem.—Eur. J.* **2007**, *13*, 7731.
(34) Grimme, S. *Org. Lett.* **2010**, *12*, 4670.
(35) Klamt, A. *Wiley Interdiscip. Rev.: Comput. Mol. Sci.* **2011**, *1*, 699.
(36) Renz, M.; Kaupp, M. *J. Phys. Chem. A* **2012**, *116*, 10629.
(37) Ess, D. H.; Houk, K. N. *J. Phys. Chem. A* **2005**, *109*, 9542.
(38) Grimme, S.; Mück-Lichtenfeld, C.; Würthwein, E.-U.; Ehlers, A. W.; Goumans, T. P. M.; Lammertsma, K. *J. Phys. Chem. A* **2006**, *110*, 2583.
(39) Dinadayalane, T. C.; Vijaya, R.; Smitha, A.; Sastry, G. N. *J. Phys. Chem. A* **2002**, *106*, 1627.
(40) Blokzijl, W.; Blandamer, M. J.; Engberts, J. B. F. N. *J. Am. Chem. Soc.* **1991**, *113*, 4241.
(41) Otto, S.; Blokzijl, W.; Engberts, J. B. F. N. *J. Org. Chem.* **1994**, *59*, 5372.
(42) Engberts Jan, B. F. N. *Pure Appl. Chem.* **1995**, *67*, 823.
(43) Fu, A.; Thiel, W. *J. Mol. Struct.: THEOCHEM* **2006**, *765*, 45.
(44) Blake, J. F.; Lim, D.; Jorgensen, W. L. *J. Org. Chem.* **1994**, *59*, 803.
(45) Chandrasekhar, J.; Shariffskul, S.; Jorgensen, W. L. *J. Phys. Chem. B* **2002**, *106*, 8078.
(46) Acevedo, O.; Jorgensen, W. L. *J. Chem. Theory Comput.* **2007**, *3*, 1412.
(47) Hu, H.; Kobrak, M. N.; Xu, C.; Hammes-Schiffer, S. *J. Phys. Chem. A* **2000**, *104*, 8058.